Electronic Supplementary Material (ESI) for Materials Advances.
This journal is © The Royal Society of Chemistry 2021

Supporting Information

Roles of Alcohols and Existing Metal Ions in Surface Chemistry and Photoluminescence of InP Cores

*Pin-Ru Chen, Kuo-Yang Lai and Hsueh-Shih Chen**

Department of Materials Science and Engineering, National Tsing Hua University, Hsinchu 30013, Taiwan

*Email: chenhs@mx.nthu.edu.tw.

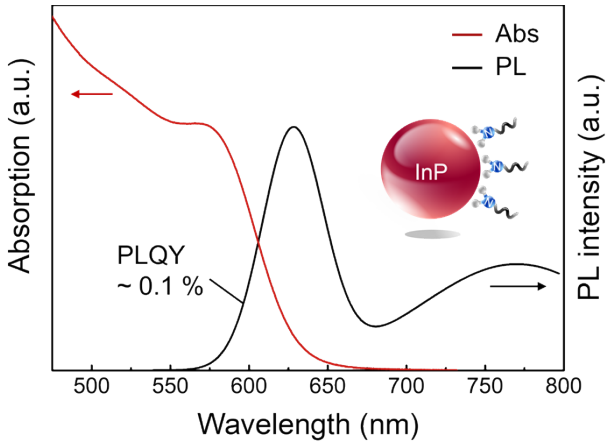

Fig. S1 Optical absorption and PL spectra of aminophosphine-based InP NCs (unwashed) that is nearly non-luminescent (PLQY ~ 0.1 %). The inset depicts the aminophosphine-based InP NCs capped with OAm as surface ligand.

Table S1 Summary of relative PL intensity, PL peak shift and absorption peak shift of InP NCs in the aging process of light/air and 168 h. The InP NCs are in a concentration of 1 mM with a total amount of 3 mL in toluene.

Aging time (h)	Relative PL intensity (%)	PL peak shift (nm)	Absorption peak shift (nm)
0	100	0	0
24	213	5	-1
48	385	-1	-8
72	412	-2	-10
168	435	-9	-21

Estimation of reaction residuals in InP and W-InP NCs.

An aliquot with a measured mass was taken out from the reaction mixture. The aliquot was then diluted with a fixed amount of toluene, and its absorbance in the short wavelength was measured. The absorbance at 413 nm along with the intrinsic coefficient of InP at the same wavelength were used to calculate the concentration of InP NCs in toluene.[1] The total amount of InP NCs in the reaction mixture was then deduced.

In the current study, approximately 0.4 mmol of InP NCs were formed in the reaction mixture with a total reaction mixture mass of 4.12 g. The molecular weight of InP is 145.8 g/mol, and 0.4 mmole InP NCs are 0.058 g. The weight ratio of InP/reaction residuals of InP NCs was approximately 1/70. The weight ratio of washed InP (W-InP) NCs was calculated from the thermogravimetric analysis (TGA). According to the TGA curve (**Fig. S2**), the solid content of InP NCs was approximately 44.6 %. Thus, the estimated InP/reaction residuals weight ratio of W-InP NCs was 1/1.2.

Furthermore, the reaction residuals can be deduced from the formed InP NCs. There was 0.4 mmol InP NCs formed in the reaction mixture, and the chemical yield is 89 %. According to literatures,[2, 3] aminophosphines would undergo a transamination with oleylamine then react with In precursors, as shown in equation (1)

$$InCl_3 + 4P(NMe_2)_3 + 12RNH_2 \rightarrow InP + 3[P(NHR)_4^+][Cl^-] + 12Me_2NH \quad (1)$$

Therefore, there may be InP, In^{3+}, Zn^{2+}, Cl^-, $P(NHR)_4^+$, Me_2NH and OAm in the reaction mixture. Me_2NH would be evaporated in the reaction mixture because of a low boiling point of it

(7 °C). The reaction residuals and their corresponding concentrations in InP NCs are listed **Table S2**. As for W-InP NC samples, the washing process would wash out most water-soluble ions including In^{3+}, Zn^{2+}, Cl^- and $P(NHR)_4^+$. **Table S3** lists the weight ratio of InP, reaction residuals, toluene and acetone in the washing process. The weight ratios of water-soluble reaction residuals in the solvent are rather low, indicating that the acetone may have enough ability to carry off most of them. According to the TGA analysis, the weight-loss region of W-InP NCs exists at the temperature higher than 200 °C, meaning most of reaction residuals are compounds with high boiling point, that may be OAm.

Table S2. List of reaction residuals and their corresponded concentration in the InP NC and W-InP NC samples.

	Weight ratio (wt %)	
	InP NCs	W-InP NCs
InP	1.3	44.6
OAm	33.4	55.4
In^{3+}	0.1	–
Zn^{2+}	3.2	–
Cl^-	4.5	–
$P(NHR)_4^+$	57.4	–

Table S3. Weight ratio of InP and reaction residuals in the washing process.

	Weight ratio (wt %)
InP	0.053
OAm	1.364
In^{3+}	0.004
Zn^{2+}	0.131
Cl^-	0.184
$P(NHR)_4^+$	2.345
Toluene	31.872
Acetone	64.047

Compared the InP NCs with W-InP NCs, the reaction residuals were largely removed by the washing process with acetone. Therefore, the effect of reaction residuals can be studied by comparing InP NCs with W-InP NCs.

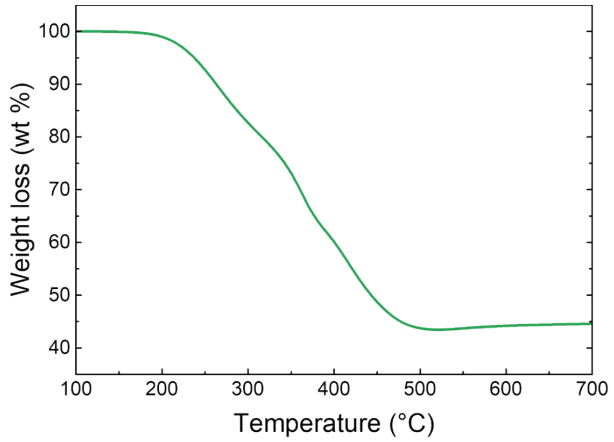

Fig. S2 Thermogravimetric analysis (TGA) of W-InP NCs to estimate the solid content of W-InP NCs and reaction residuals.

Material properties of of InP and W-InP NCs

It should be noted that the InP NCs used in the aging process are those collected directly from the reaction mixture without any washing process. Thus, we could only measure the optical absorption and PL spectra of InP NCs. For other analyses, such as XRD, TEM and TGA, which may need the samples in a purified condition, meaning the NCs with less reaction residuals and surface ligands, it may have difficulty to obtain these data of InP NCs.

Fig. S3 shows the XRD pattern, TEM image and atomic ratio of W-InP NCs acquired from ICP-MS analysis. The XRD patterns of W-InP NCs are well-indexed to InP cubic structure. According to TEM images, the average size of W-InP NCs is 2.6 ± 0.4 nm. Furthermore, the W-InP NC diameter calculated according to a sizing curve (equation (2) and (3)) in reference of previous literatures is also 2.6 nm,[4-7] that is in good agreement with TEM analysis where d_{NC} is the diameter of NC (in nm), λ is the absorption peak (in nm) of NCs and E_g is the band gap energy (in eV).

$$d_{NC} = 0.1456 \times e^{0.0052 \cdot \lambda} \tag{2}$$

$$E_g = 1.35 + \frac{1}{(0.119 \pm 0.003) d_{NC}^2} \tag{3}$$

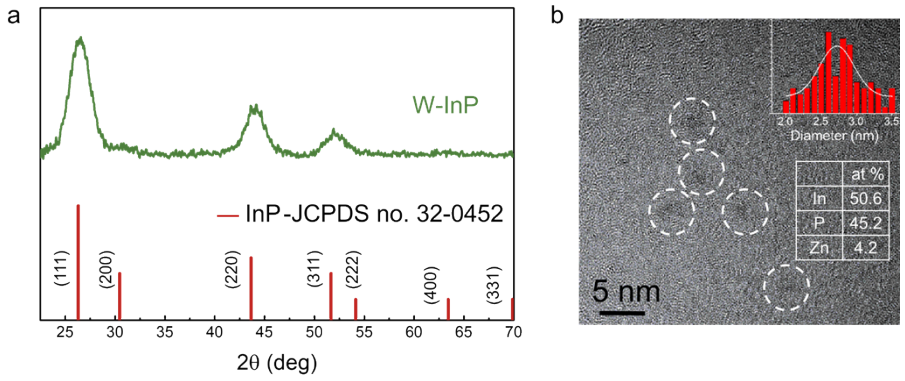

Fig. S3 (a) XRD patterns and (b) TEM images of W-InP NCs. The XRD patterns of W-InP NCs are well-indexed to InP cubic structure, indicating there may be no structural change after the washing process. The W-InP NC size calculated from TEM images is 2.6 ± 0.4 nm. The insets in (b) show the size distribution of W-InP and atomic composition of W-InP NCs acquired from ICP-MS analysis.

According to TEM images and InP sizing curves from literatures,[4-7] aged InP NCs generally show the blueshift of 3-20 nm in absorption peaks, corresponded to a reduction of 0.05-0.2 nm in the NC size. The W-InP NCs aged in light/air for 48 h with the largest blueshift of 48 nm in absorption peak, corresponded to a reduction of ~ 0.5 nm in the NC size calculated from sizing curve. However, low Z-contrast and small size of InP NCs make observation of NC size and morphology changes difficult through TEM analysis with limit resolution. In addition, the NC surface oxidation may generate an oxidation layer with reduced NC size, that may lead to a similar NC size before and after oxidation. Therefore, the InP NC oxidation in the current study is mainly investigated by NC optical properties and XPS analysis.

Table S4 Summary of optical characteristics of InP and W-InP NCs aged under light/Ar, light/air, dark/air and dark/Ar for 48 h. All samples are in a concentration of 1 mM with a total amount of 3 mL in toluene.

	InP		W-InP	
	Relative PL intensity (%)	Absorption peak blueshift (nm)	Relative PL intensity (%)	Absorption peak blueshift (nm)
light/Ar	260	7	187	18
light/air	392	12	40	48
dark/Ar	191	3	169	3
dark/air	222	3	171	3

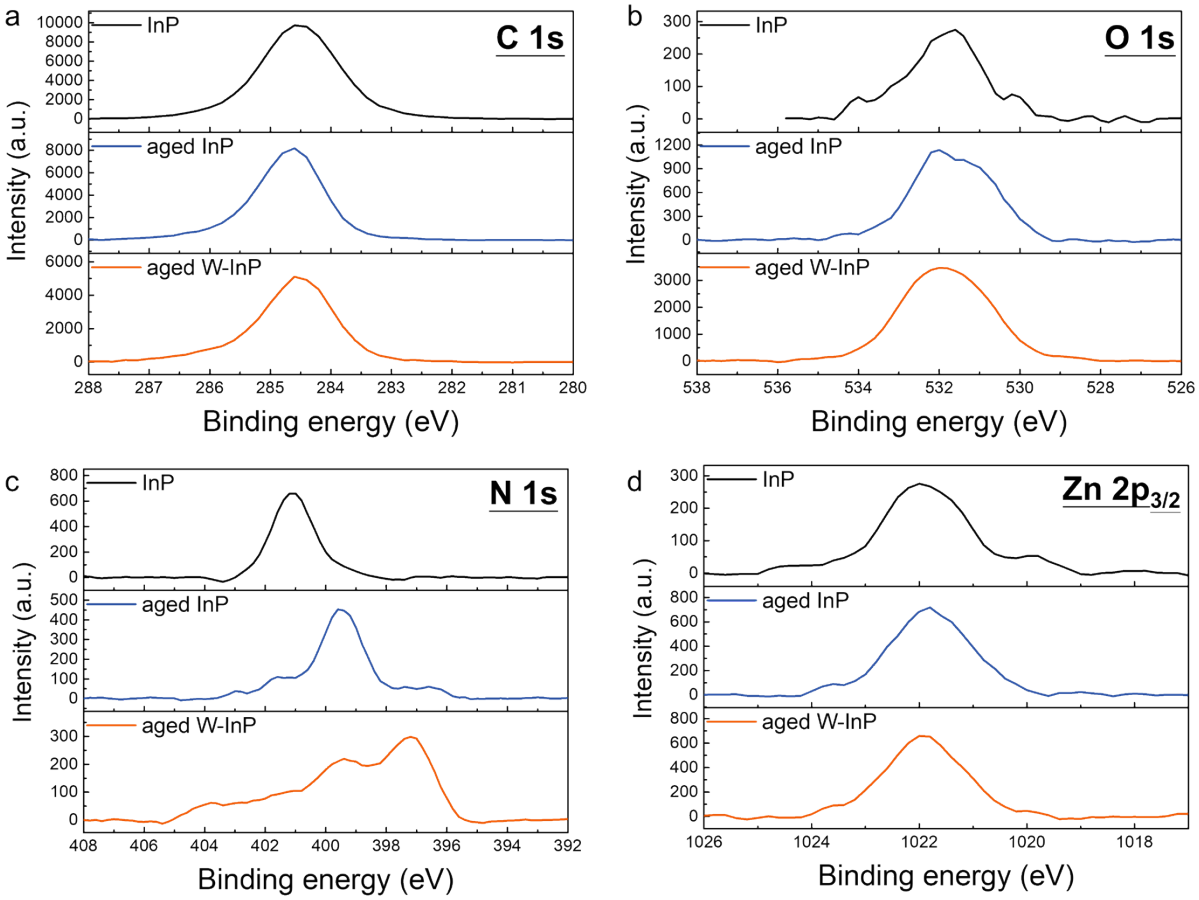

Fig. S4 XPS C 1s, O 1s, N 1s and Zn $2p_{3/2}$ spectra of InP, aged InP and aged W-InP. The XPS spectra are further used to calculate the relative atomic ratio of each elements by relative sensitivity factor (RSF).

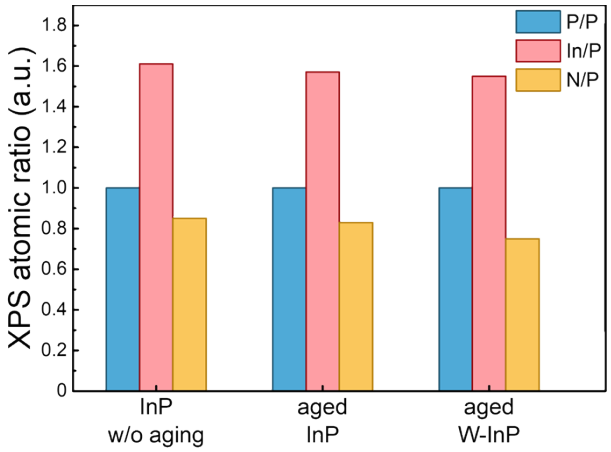

Fig. S5 XPS In/P and N/P atomic ratio of InP, aged InP and aged W-InP NC samples calculated from corresponding XPS spectra. The aged samples are aged in light/air for 48 h. All atomic ratios are presented relative to P while the ratio of P is fixed to 1.

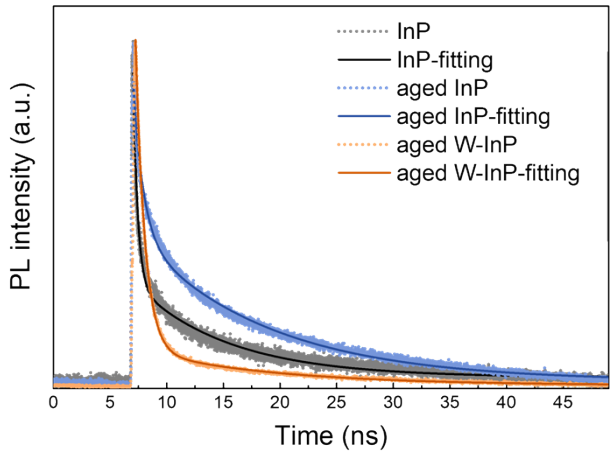

Fig. S6 Time-resolved PL (TRPL) spectra of InP, aged InP and aged W-InP NC samples. The PL decay curves can be fitted with a bi-exponential function: $I(t) = A_1\exp\left(\frac{-t}{\tau_1}\right) + A_2\exp\left(\frac{-t}{\tau_2}\right)$, where I is the PL intensity at time t, A_1 and A_2 are weight constants, $A_1 + A_2 = 1$, and τ_1 and τ_2 are time constants for the exponential components. The weighted PL lifetime (τ_{av}) can be determined by the expression: $\tau_{av} = (A_1{\tau_1}^2 + A_2{\tau_2}^2)/(A_1\tau_1 + A_2\tau_2)$. The short-lifetime component (τ_1) with higher amplitude is ascribed to band-edge emission while the long-lifetime component (τ_2) with lower amplitude is assigned to surface defect states.[8, 9] The PL lifetime of InP, aged InP and aged W-InP are 5.77, 10.54 and 6.73 ns, respectively. The increased PL lifetime of aged InP NC sample suggest that the $InPO_x$ oxidation indeed passivate NC surface. The increased amplitude of A_2 also implies formation of additional radiative defects on InP NC surface. In the case of aged W-InP NC sample, an apparently distinct decay curve with increased lifetime of long-lifetime component is observed. The strong oxidation of W-InP NC sample would create both non-radiative and radiative state with a comparable PL lifetime as that of InP NC sample.

Table S5 Fitting parameters for TRPL decay dynamics in InP, aged InP and aged W-InP NC samples.

Sample	A_1	τ_1 (ns)	A_2	τ_2 (ns)	Weighted τ_{av} (ns)
InP	0.91	0.39	0.09	8.32	5.77
aged InP	0.61	0.88	0.39	11.67	10.54
aged W-InP	0.93	0.82	0.07	11.98	6.73

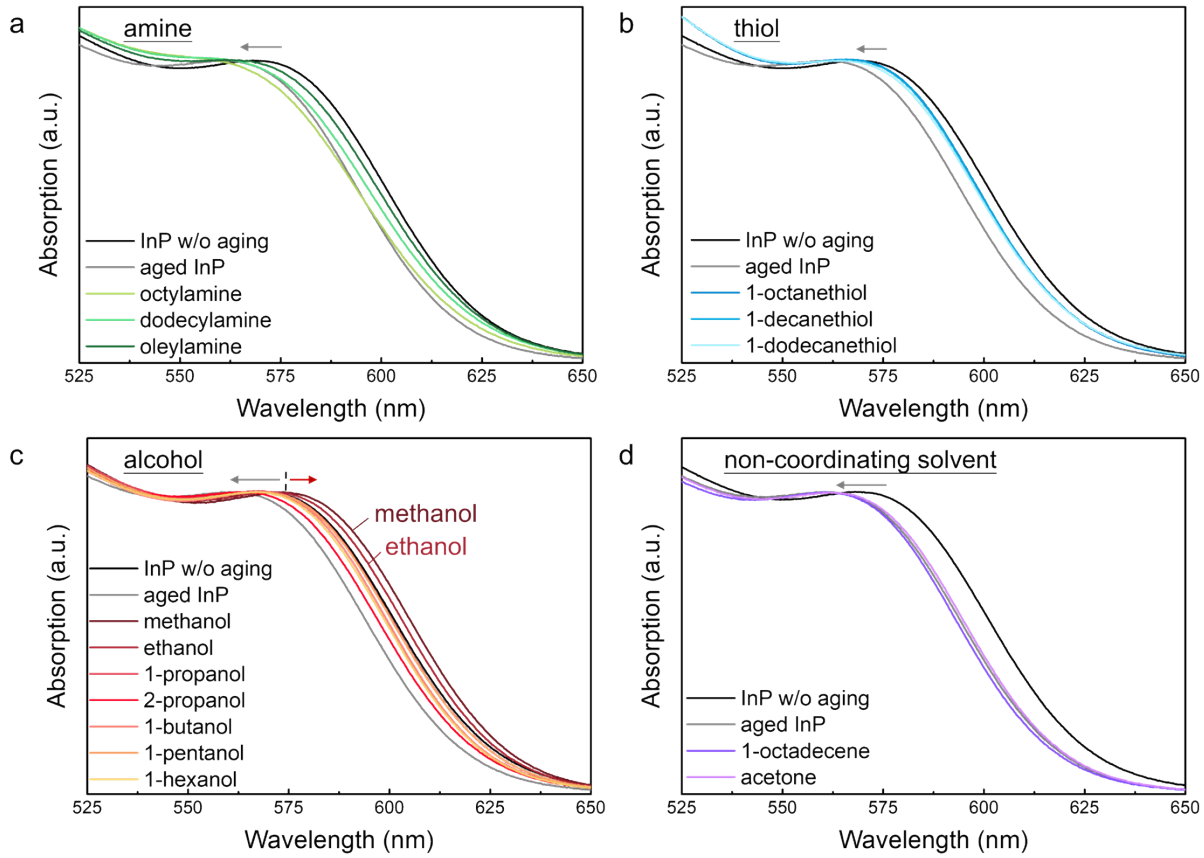

Fig. S7 Effect of additives on InP NC oxidation in the aging process. Optical absorption spectra of InP NCs after aging in light/air for 48 h with different additives. All samples are in a concentration of 1 mM with a total amount of 3 mL in toluene. (a) Amine-additives (octylamine, dodecylamine and oleylamine). (b) Thiol-additives (1-octanethiol, 1-decanethiol and 1-dodecanethiol). (c) Alcohol-additives (methanol, ethanol, 1-propanol, 2-propanol, 1-butanol, 1-pentanol and 1-hexanol). (d) 1-octadecene-additive and acetone-additive.

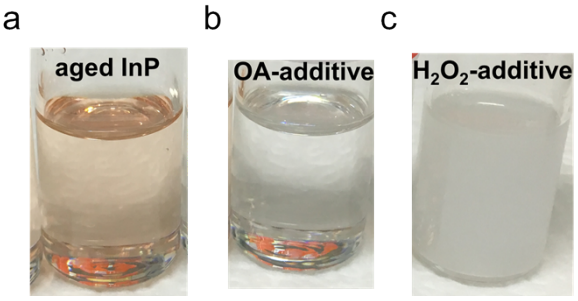

Fig. S8 Photographs of InP NC sample solutions after aging in light/air for 48 h. (a) Aged InP NC sample without any additive still shows a light-orange color. (b) OA- and (c) H_2O_2-additive samples in which OA-additive sample becomes transparent and H_2O_2-additive sample turns into a turbid solution. All samples are in a concentration of 1 mM with a total amount of 3 mL in toluene.

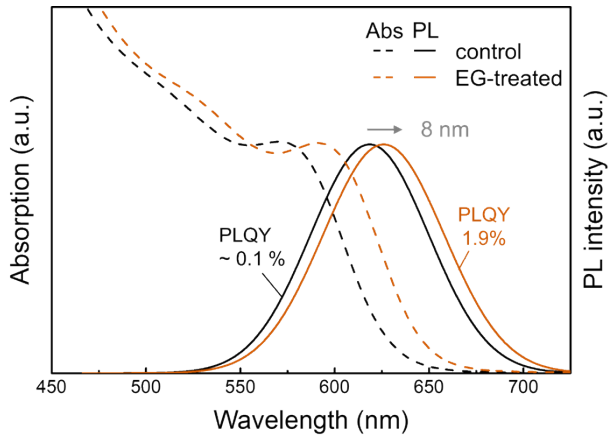

Fig. S9 EG treatment of InP NCs. Optical absorption and PL spectra of the control sample (treated with acetone) and EG-treated InP NCs. The immiscibility of EG and InP/toluene solution shows that reaction between high polarity solvent and InP NCs occurs rapidly that only needs a simply stirring to induce PL enhancement.

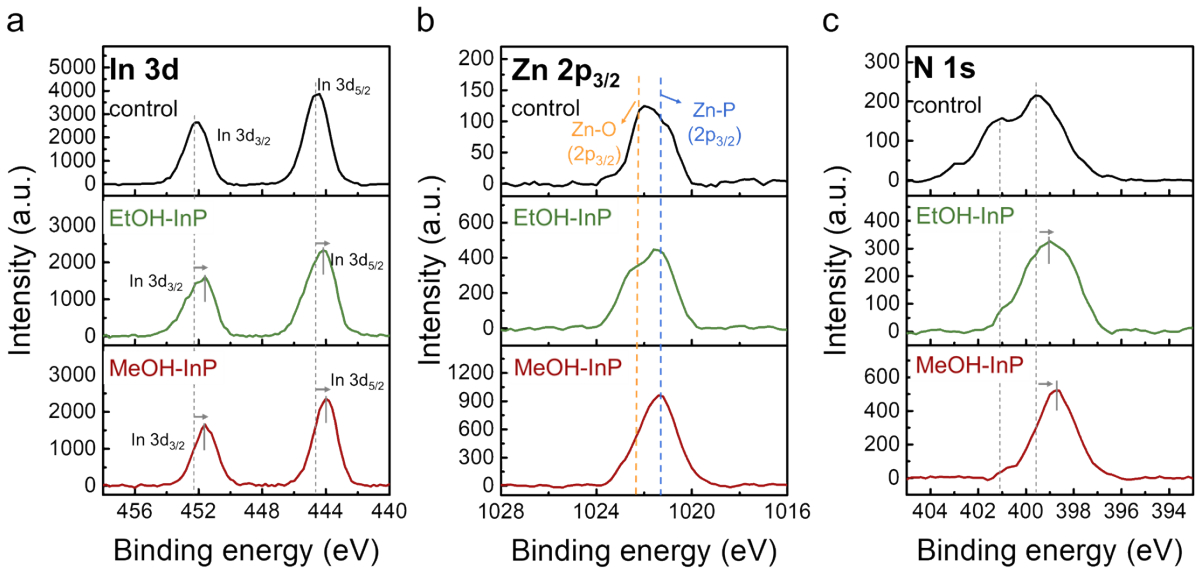

Fig. S10 XPS (a) In 3d, (b) Zn $2p_{3/2}$ and (c) N 1s spectra of the control, ethanol- and methanol-treated InP NC samples. Both In $3d_{3/2}$ and In $3d_{5/2}$ of EtOH- and MeOH-InP NCs shift toward lower binding energy that may indicate more OAm bind to InP NC surface. The formation of $Zn_yIn_{1-y}PO_x$ oxide layer would result in increased In-PO_x with the peaks shifting to higher binding energy; however, the effect of increased In-N bonds is larger than increased In-PO_x bonds for the overall peak shifting to lower binding energy. A low Zn content is observed in the control sample. Zn contents increase after alcohol treatment for both EtOH- and MeOH-InP NCs with similar Zn $2p_{3/2}$ peak position. Both Zn-O and Zn-P bonds existing in $Zn_yIn_{1-y}PO_x$ layer could be observed in the alcohol-treated Zn $2p_{3/2}$ spectra. The control sample exhibits a shoulder around 401 eV in N 1s spectrum probably originated from some protonated OAm. After the alcohol treatment, the N 1s peaks of both EtOH- and MeOH-InP NCs shifting toward lower binding energy with increased N content may suggest better surface passivation and redshifted spectral peaks of alcohol-treated InP NCs.

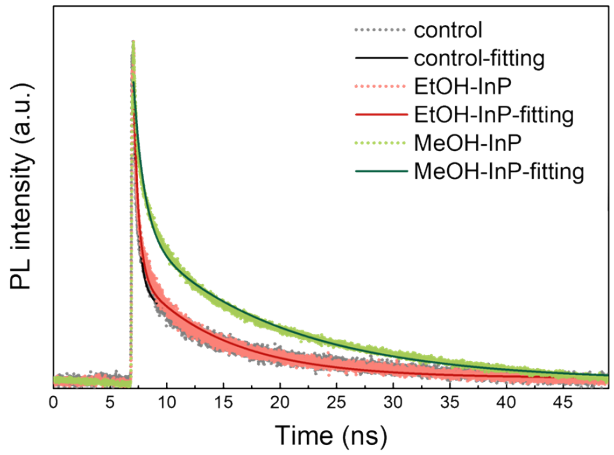

Fig. S11 TRPL spectra of control, EtOH- and MeOH-InP NC samples. The PL lifetime are 5.77, 6.26 and 11.48 ns of control, EtOH- and MeOH-InP NC samples, respectively. The both increased PL lifetime of EtOH- and MeOH-InP NC samples suggest better surface passivation of InP NCs after the alcohol treatment. An increased amplitude in τ_2 suggest that $Zn_yIn_{1-y}PO_x$ oxidation layer would create surface radiative states and thus responsible for the both PL and optical absorption peak redshift.

Table S6 Fitting parameters for TRPL decay dynamics in control, EtOH- and MeOH-InP NC samples.

Sample	A_1	τ_1 (ns)	A_2	τ_2 (ns)	Weighted τ_{av} (ns)
Control	0.91	0.39	0.09	8.32	5.77
EtOH-InP	0.83	0.44	0.17	7.86	6.26
MeOH-InP	0.60	0.94	0.40	12.67	11.48

REFERENCES

(1) Aspnes, D. E.; Studna, A. A., Dielectric Functions and Optical-Parameters of Si, Ge, Gap, Gaas, Gasb, Inp, Inas, and Insb from 1.5 to 6.0 eV. *Phys. Rev. B* **1983,** *27,* 985-1009.
(2) Tessier, M. D.; De Nolf, K.; Dupont, D.; Sinnaeve, D.; De Roo, J.; Hens, Z., Aminophosphines: A Double Role in the Synthesis of Colloidal Indium Phosphide Quantum Dots. *J. Am. Chem. Soc.* **2016,** *138,* 5923-5929.
(3) Buffard, A.; Dreyfuss, S.; Nadal, B.; Heuclin, H.; Xu, X. Z.; Patriarche, G.; Mezailles, N.; Dubertret, B., Mechanistic Insight and Optimization of InP Nanocrystals Synthesized with Aminophosphines. *Chem. Mater.* **2016,** *28,* 5925-5934.
(4) Xie, R. G.; Li, Z.; Peng, X. G., Nucleation Kinetics vs Chemical Kinetics in the Initial Formation of Semiconductor Nanocrystals. *J. Am. Chem. Soc.* **2009,** *131,* 15457-15466.
(5) Crisp, R. W.; Kirkwood, N.; Grimaldi, G.; Kinge, S.; Siebbeles, L. D. A.; Houtepen, A. J., Highly Photoconductive InP Quantum Dots Films and Solar Cells. *ACS Appl. Energy Mater.* **2018,** *1,* 6569-6576.
(6) Micic, O. I.; Ahrenkiel, S. P.; Nozik, A. J., Synthesis of Extremely Small InP Quantum Dots and Electronic Coupling in Their Disordered Solid Films. *Appl. Phys. Lett.* **2001,** *78,* 4022-4024.
(7) Micic, O. I.; Curtis, C. J.; Jones, K. M.; Sprague, J. R.; Nozik, A. J., Synthesis and Characterization of InP Quantum Dots. *J. Phys. Chem.* **1994,** *98,* 4966-4969.
(8) Fitzmorris, B. C.; Cooper, J. K.; Edberg, J.; Gul, S.; Guo, J. H.; Zhang, J. Z., Synthesis and Structural, Optical, and Dynamic Properties of Core/Shell/Shell CdSe/ZnSe/ZnS Quantum Dots. *J. Phys. Chem. C* **2012,** *116,* 25065-25073.
(9) Pal, A.; Srivastava, S.; Gupta, R.; Sapra, S., Electron transfer from CdSe-ZnS core-shell quantum dots to cobalt(III) complexes. *Phys. Chem. Chem. Phys.* **2013,** *15,* 15888-15895.